electronics

Article

Accumulation and Elimination: A Hard Decision-Based Multi-User Interference Cancellation Method in Satellite Communication System

Haohan Li [1,2], Yongjia Jin [1], Deguang Zhao [3], Xuhui Ding [2,3,*] and Kai Yang [1]

[1] School of Information and Electronics, Beijing Institute of Technology, Beijing 100081, China; lihaohan@bit.edu.cn (H.L.); jinyongjia@bit.edu.cn (Y.J.); yangkai@bit.edu.cn (K.Y.)
[2] Yangtze Delta Region Academy, Beijing Institute of Technology, Jiaxing 314019, China
[3] School of Cyberspace Science and Technology, Beijing Institute of Technology, Beijing 100081, China; zhaodeguang@bit.edu.cn
* Correspondence: dingxuhui@bit.edu.cn

Abstract: With the increasing number of users in the Medium-Orbit (MEO) satellite communication system, multi-access interference (MAI) has become an important factor that restricts the reliability and capacity of the system. Additionally, the low carrier-power-to-noise-density ratio (C/N_0) resulting from long-distance transmission poses a significant concern. The parallel interference cancellation (PIC) algorithm, utilized within the paradigm of multi-user detection (MUD), exhibits the capability to effectively mitigate the impact of MAI within the same system. Simultaneously, coherent accumulation serves as a means to substantially enhance the correct detection probability (P_{cd}) at low C/N_0. In this study, a signal acquisition method for multi-user spread spectrum satellite receivers is proposed, which employs interference cancellation and coherent accumulation as its core mechanisms. Furthermore, we introduce a power estimation method based on the outcomes of signal acquisition, which can be integrated into the signal reconstruction module of PIC. Finally, we implement the aforementioned algorithms in both simulation and hardware platforms. Remarkably, we observe that when the interference-to-signal ratio (ISR) caused by MAI equals 20 dB, the improved algorithm attains a maximum P_{cd} of 0.95 within the high signal-to-noise ratio (SNR) region, closely approaching the theoretical limit for the bit error rate (BER). The experimental results prove the effectiveness and feasibility of the acquisition algorithm. In summary, the enhanced algorithm holds vast potential for widespread implementation in multi-user spread spectrum communication systems.

Keywords: Code Division Multiple Access; direct sequence spread spectrum; parallel interference cancellation; coherent accumulation; acquisition

Citation: Li, H.; Jin, Y.; Zhao, D.; Ding, X.; Yang, K. Accumulation and Elimination: A Hard Decision-Based Multi-User Interference Cancellation Method in Satellite Communication System. *Electronics* **2023**, *12*, 4878. https://doi.org/10.3390/electronics12234878

Academic Editor: Silvia Liberata Ullo

Received: 9 November 2023
Revised: 26 November 2023
Accepted: 27 November 2023
Published: 4 December 2023

1. Introduction

With the rapid advancement of aerospace technology, satellite communication networks have garnered escalating attention from myriad industries. Among them, the Earth Medium Orbit Satellite (MEO) communication system has found extensive utilization across numerous countries and systems. Prominent examples include the BeiDou-3 short message communication system and the Global Positioning System (GPS) communication system, which has seen continuous development over the years. Both of these systems employ MEO satellites as a foundation to fulfill the need for worldwide communication coverage with a minimal number of constellations. MEO systems can provide extensive communication range and are capable of withstanding severe environmental conditions. Despite the limitation of 120 Chinese characters per transmission, these systems facilitate the exchange of information among terminals and enable effective communication and connectivity [1]. Concurrently, the aforementioned system implements direct sequence spread spectrum and code division multiple access (DS-CDMA) technologies to elevate system capacity for the increasing number of users and the limited spectrum resources. Due to these advantages, the MEO communication system has proven to be successful when ground communications services fail or cannot reach. For example, in pelagic fishery, earthquake rescue, forest fire monitoring, location monitoring of international flights, or unmanned aerial vehicles (UAVs) [2–4].

However, with the increase in the number of users, the concern for multi access interference (MAI) becomes more compelling within DS-CDMA systems [5]. MAI exists when a weak received signal is interfered with by one or more strong signals as expounded in [6,7]. As a result, the effective cross-correlation among signals weaken the communication capability of the up-link satellite receiver, which is shown in Figure 1. Despite the insignificant effect that an individual user may have on others, the proliferation of synchronous signals amplifies the impact of MAI, thereby considerably impacting communication stability significantly. We must highlight that current acquisition algorithms cannot solve the MAI problem [6], thus illuminating the requirement for innovative solutions.

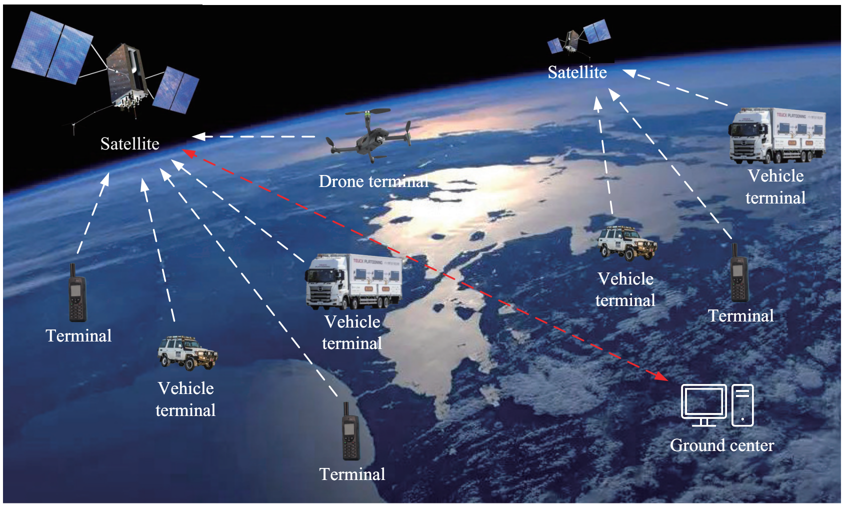

Figure 1. The up-link of the multi-user system.

In DS-CDMA systems, the signals of all users overlap in both time and frequency dimensions. Conventional DS-CDMA systems follow a single-user detection strategy, where users are detected by correlating the received signals with the local pseudo-noise (PRN) codes through a specific filter, known as the matched filter method [8,9]. In reference [10], Choi presented a method to capture weak signals in the presence of strong interference, irrespective of signal power, noise power, and jamming power. In reference [11,12], they considered methods to eliminate narrow-band interference as well as broad-band interference to improve acquisition performance. In reference [13], the proposed algorithm decreases the false alarm probability through the decision of the ratio of the maximum value and the second maximum value of the correlation results. However, none of the aforementioned methods took MAI into consideration.

MAI greatly affects the individual detection results. In reference [14], multi-user detection algorithms (MUD) were introduced as a promising solution to address this problem. In reference [15], Xie proposed a class of suboptimal detectors based on the minimization of the mean square error (MMSE) or the weighted-squared-error performance criterion. Although these detectors perform nearly as well as the optimal detector, their utilization is hindered by the impracticality of real-time matrix inverse operations [16]. To mitigate the computational complexity, interference-canceling multi-user detection algorithms have been developed and put forward. As discussed in [17–19], serial interference cancellation (SIC) possesses the capability to eliminate not only the signals transmitting from other users within the same communication system but also the pernicious narrow-band interference. Nevertheless, the SIC algorithm demands a significant level of power control, and its serial nature cannot meet the real-time acquisition requirements. In reference [20], the multi-stage parallel interference cancellation (PIC) algorithm concurrently analyzes all MAI for simultaneous cancellation, which can additionally be cascaded for utmost optimization. The utilization of a lower number of layers facilitates rapid processing capabilities. Among various MUD algorithms, PIC is particularly well suited for the acquisition module of receivers.

In addition, the MEO satellite communication system faces the issue of a low carrier-to-noise ratio (C/N_0) due to various factors. One of the main reasons is that MEO satellites are typically located around 20,000 km away from the ground, which causes serious propagation attenuation [21,22]. Consequently, signal acquisition becomes a difficult task for the receiver. With the development of DSP technology, contemporary spread spectrum receivers have embraced fast acquisition algorithms rooted in the Fast Fourier Transform (FFT). In reference [23,24], they introduced a rapid acquisition algorithm founded on FFT, which effectively estimates the Doppler shift during the PRN phase acquisition. In reference [25], Yang discussed the performance of weak GPS signal acquisition algorithms from executive time and detection possibility. The findings indicate that coherent accumulation exhibits superior detection capabilities and expeditious processing velocity. In reference [26], Tang proposed a low-complexity acquisition algorithm that is capable of capturing extremely weak direct sequence spread spectrum (DSSS) signals. They discussed coherently accumulating the correlation results across multiple PRN code periods to achieve a reliable signal–noise ratio (SNR) for acquisition. We consider the application of the coherent accumulation algorithm in the MAI scenario and use it as the main comparison object for this scenario.

This paper investigates the acquisition algorithm designed for on-board receivers installed on MEO satellites. This study specifically takes into account the challenging conditions of MAI and puts forth an improved acquisition algorithm rooted in coherent accumulation and PIC. Furthermore, we propose a hard reconstruction method based on the acquisition results. Subsequently, the performance of the proposed algorithm is analyzed, highlighting its notable attributes, which include fast acquisition, high detection probability, and effective reduction of BER. Finally, the hardware architecture is presented, and the results of the experiment are discussed. The outcomes of this research hold broad applicability within DS-CDMA communication systems, finding utility in both MEO and Low Earth Orbit (LEO) satellite systems.

2. Influence of MAI on Acquisition Module

2.1. Mathematical System Model of Synchronous DS-CDMA Channel

In this section, we take a more detailed look at the influence of MAI on the DS-CDMA system, particularly focusing on the acquisition module. It is imperative to define the mathematical model. We assume that the system contains a total of K users as shown in Figure 2. Initially, the unprocessed data from each user are converted by pairwise polarization. Subsequently, the polarized data are subject to spread spectrum coding, utilizing a local PRN code generated by a circular shift register. Following this, modulation into the Radio Frequency (RF) band is employed. Ultimately, the spread spectrum signals of all users are transmitted to the receiver via a Gaussian channel after aliasing.

The aliased multi-user signal, which arrives at the on-board receiver, is denoted as

$$y_{in}(iT_s) = \sum_{n=1}^{K_{user}} A_n b_n[i] c_n(iT_s - \tau_n) e^{j2\pi(f_r + f_d^n)iT_s} + n_o(iT_s), \quad (1)$$

where

$K_{user} = 1, 4, ..., 16$ is the number of user signals arriving at the on-board receiver.
$A_n > 0$ is the signal amplitude of user n.
$b_k() \in [1, -1]$ is the unprocessed data sent by user n.
$c_k()$ is the PRN spreading sequence code used by user n.
$T_S = \frac{1}{f_s}$ is the system sampling period.

f_s is the system sampling rate.
τ_n is the initial phase of the PRN code for user n.
f_r is the carrier RF point, every user in the system share the same f_r.
f_d^n is the carrier Doppler frequency offset for user n.
$n_0(iT_s)$ is the additive Gaussian white noise with mean 0 and variance σ_n^2.

Here, we need to point out that data modulation might be inconvenient for the coherent accumulation algorithm. So, we assume that each transmitter sends a non-data-modulated section before its information-bearing segment in every burst frame [27], which is abbreviated as

$$y_{in}(iT_s) = \sum_{n=1}^{K_{user}} A_n c_n(iT_s - \tau_n) e^{j2\pi f_d^n iT_s} + n_o(iT_s). \tag{2}$$

This study aims to explore the up-link receiver acquisition problem in a multi-user system, utilizing the aforementioned signal models as the foundation. Equation (1) is employed in the analysis of the transmission outcome to simulate the bit error rate (BER). Equation (2) is employed in the analysis of the acquisition module to simulate the correct detection probability (P_{cd}).

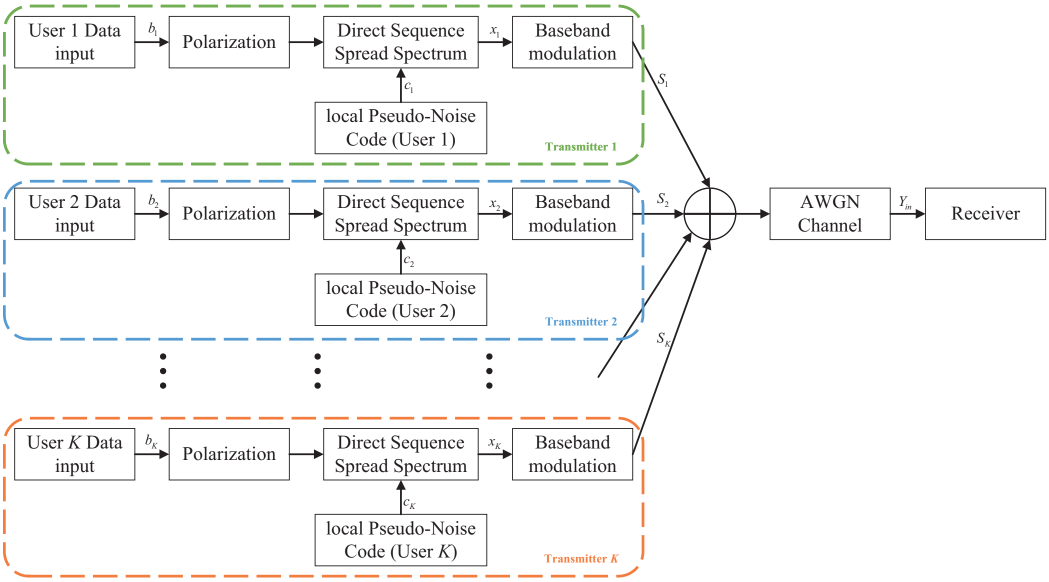

Figure 2. Transmitter.

2.2. The Influence of MAI

In this subsection, we will analyze the interference experienced by weak signals arising from other users within the system. In MEO communication systems, the free space loss determined by the transmission distance from the ground terminals to the satellite is the main loss suffered by signals, which is defined as

$$L_f = 20\lg\frac{4\pi d f_r}{c}(\text{dB}), \tag{3}$$

where

f_r is the carrier RF point, and 1.6 Ghz is taken in this paper.
c is the speed of light, and 3×10^8 m/s is taken in this paper.
d is the actual transmission distance of the user's signal.

In our analysis, we assume the altitude of MEO satellites is 21,500 km, which means that the transmitter closest to the satellite experiences a loss of L_{f1} equal to 183.1729 dB, while the furthest transmitter suffers a loss of L_{f2} equal to 185.1959 dB.

Although the interference caused by a strong user towards a weak user is merely 2 dB, the increasing number of transmitters results in an amplified presence of interference within the received signals. This leads to a serious performance degradation of the receiver system, impeding its ability to accurately capture the time and frequency bias information from each user. The subsequent functioning of the receiver is also influenced as depicted in Figure 3.

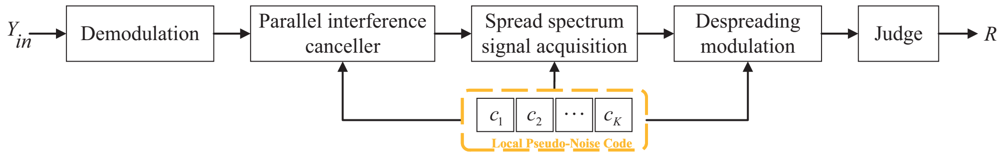

Figure 3. Receiver.

Figure 4 illustrates the MAI experienced by weak signals with the number of strong signals increasing, quantified through the interference-to-signal ratio (ISR).

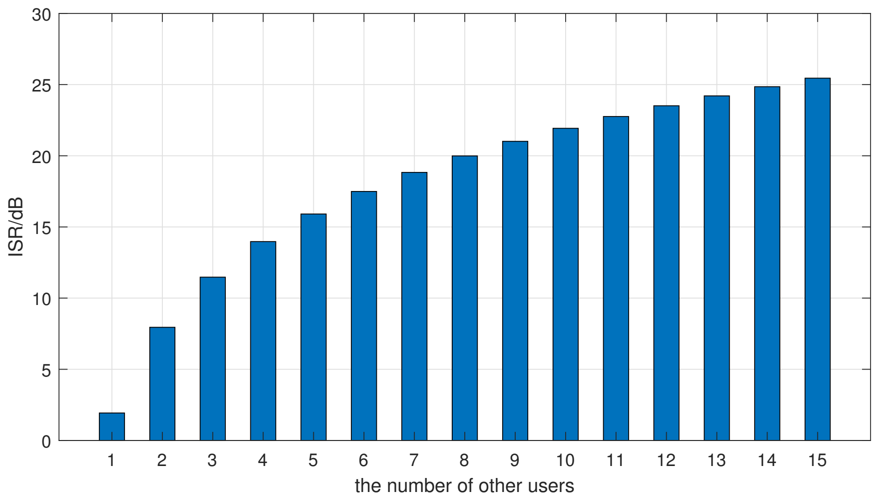

Figure 4. MAI suffered by weak signal.

3. The Acquisition Method Based on PIC

3.1. The Improved Algorithm Based on PIC and Coherent Accumulation

In this subsection, we will focus on the presentation of the proposed acquisition algorithm based on the MUD algorithm and coherent accumulation algorithm. Given that MAI holds significant influence over the performance and capacity of multi-user systems, the interference cancellation algorithms can effectively mitigate its impact. Furthermore, coherent accumulation can significantly improve the acquisition performance in low-SNR scenarios. The improved algorithm is based on the following idea.

As shown in Figure 3, the received signal first undergoes the parallel K-user acquisition module. From this module, we obtain the time bias and frequency bias information of all users. It should be noted that we optimize the coherence peaks of received signals here using the coherent accumulation module. Subsequently, reconstruction is carried out based on the aforementioned information of the strong signals. Simultaneously, by subtracting the reconstructed interfering signal from the original received signal, we can effectively eliminate the MAI. The detailed algorithm for reconstructing the interference signal will be explained in Section 3.3 of this paper.

In DS-CDMA systems, the PIC method can be regarded as a practical multi-user detection technique that strikes a balance between algorithmic performance and complexity. Because of the reduced reliance on power control and MAI elimination order, PIC, surpassing SIC, is more efficient in eliminating interference. Consequently, PIC becomes the more suitable method for implementation within acquisition modules, enhancing system detection efficiency. Figure 5 exemplifies one stage of the PIC-based acquisition algorithm.

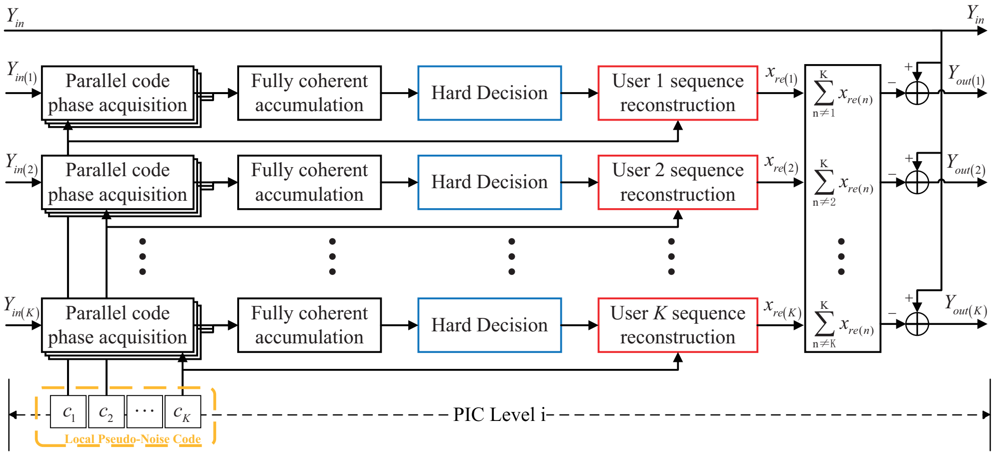

Figure 5. Single-stage PIC processing flow.

Further analysis of the on-board receiver is also required. As expounded in Section 2.1, we mainly focus on acquisition methods for non-data-modulated segments. Thus, it becomes more convenient to estimate the power of the received signal and eliminates the issue of bi-phase ambiguities, which occurs when the received sequence occupies half of the front and back PRN codes.

The specific flow of the PIC-based spread spectrum acquisition algorithm is delineated as follows.

(1) Initially, the demodulated received signal $y_{in}(iT_s)$ is concurrently fed to independent acquisition modules for K users. Through correlating $y_{in}(iT_s)$ with individual user's local PRN code and accumulating the outcomes, a comprehensive two-dimensional search, including time and frequency for K groups is executed. The obtained outcomes are defined as $z_1(n,m), z_2(n,m), ..., z_K(n,m)$.

(2) By identifying the maximum correlation value within the aforementioned search results, with its corresponding frequency and time deviations, the signal for each user is $x^1\hat{(k)}, x^2\hat{(k)}, ..., x^K\hat{(k)}$. Subsequently, the reconstructed signals, except the target user, are accumulated. This summation enables the extraction of all the MAI information associated with the target user.

(3) By subtracting the previously reconstructed MAI from the original input signal, the interference-canceled signals $y_{out}(iT_s)$ are obtained. Following this, another round of acquisition operation is conducted for all users to obtain the interference-canceled K-group time-frequency two-dimensional search results $z_1(\hat{n},m), z_2(\hat{n},m), ..., z_K(\hat{n},m)$. At this stage, a significant portion of the MAI is effectively eliminated, while simultaneously enhancing the prominence of peaks corresponding to weak signals. As a result, P_{cd} is substantially increased.

(4) Steps 1–3 constitute one stage of the PIC-based acquisition module. Furthermore, it is feasible to put the output signal from step 3 into another stage of the PIC module. By repeating steps 2 and 3, MAI can be further diminished, consequently leading to an enhancement in the detection performance of the system.

3.2. Design of the Coherent Accumulation Module

In this subsection, we discuss the coherent accumulation algorithm employed in this paper. Our objective is to accumulate the correlation outcomes of various symbols, thereby augmenting the correlation between the target signal and the local PRN code as proposed in [26].

Figure 6 illustrates the overall process of the coherent accumulation algorithm. Firstly, the received signal y_{in} is inputted into the parallel code phase acquisition module, which operates in frames. When processing a specific frame, the y_{in} is shifted after being passed through FFT to simulate sequences under different frequency offsets. The local PRN code is conjugated after being subjected to FFT, and the two sequences are multiplied together to obtain the correlation result. The results of m frames are stored for future processing. Then, through multiple instances of correlation and coarse Doppler compensation using FFT, the correlation outcomes from the m sets of acquisition results are accumulated utilizing FFT for processing. This accumulation process can be expressed as

$$z(n,m,w) = \sum_{v=1}^{V} z'(n,m,v)e^{-j\frac{2\pi}{W}wV}. \tag{4}$$

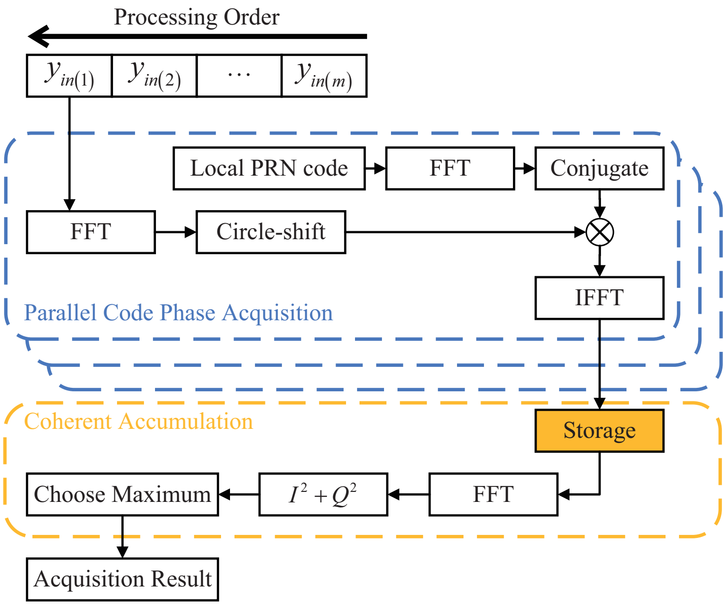

Figure 6. Block diagram of the coherent accumulation acquisition algorithm.

For low-complexity considerations, we choose the highest value in the outcomes as the output representing the correlation peak.

It is worth noting that the quantity of symbols employed for accumulation impacts the ultimate correlation peaks. In low-SNR scenarios, we are inclined to employ the longest feasible sequence for accumulation, but this may result in a too-long processing time. Thus, the selection of the sequence length used for accumulation needs deliberate design.

3.3. Design of the Hard Reconstruction Module

As shown in Figure 5, the hard decision module and the reconstruction module serve as the fundamental pillars of the aforementioned PIC-based acquisition algorithm. The reconstructed signal directly affects the effectiveness of interference cancellation. In this paper, we propose a method to estimate the amplitude of strong signals based on the acquisition results, which can augment the efficacy of PIC in eliminating interference signals.

First, the hard decision module necessitates estimating the amplitude of the received signal. So, we discuss the the correlation between the reconstructed signal sequence and the received signal. The reconstructed sequence is delineated as

$$x(\hat{k}) = Re_{coef} \times x(k), \tag{5}$$

where $x(k) = b_n c_n$ is the non-data-modulated spread spectrum sequence, and Re_{coef} is the predicted coefficient of the reconstructed sequences.

The power of the reconstructed signal is

$$\hat{P_{Re}} = Re_{coef}^2 \times \sum_{k=0}^{N-1} x^2(k). \tag{6}$$

The objective of the reconstruction module is to minimize the disparity between the estimated parameter Re_{coef} and the received signal amplitude A_n. Thus, we direct our focus towards the aforementioned parameters. The results of the acquisition algorithm manifest as a correlation between the received signal and the localized PRN code, which is defined as

$$z(n,m) = \sum_{k=0}^{N-1} x(k) y_{in}(k-n,m). \tag{7}$$

In the event of a successful acquisition, there are values N and M such that $z(N,M)$ achieves the maximum value denoted as z_{max}. Precisely, z_{max} indicates the position where the local PRN code sequence exhibits the highest correlation value with the received signal sequence:

$$\begin{aligned} z_{max} &= \sum_{k=0}^{N-1} x(k) y_{in}(k) \\ &= \sum_{k=0}^{N-1} x(k)[A_n x(k) + n_0] \\ &= \sum_{k=0}^{N-1} A_n x^2(k) + \sum_{k=0}^{N-1} x(k) n_0. \end{aligned} \tag{8}$$

The power information of the reconstructed signal is further derived from the above equations:

$$A_n = \frac{z_{max} - \sum\limits_{k=0}^{N-1} x(k) n_0}{\sum\limits_{k=0}^{N-1} x^2(k)}. \tag{9}$$

Since Gaussian white noise is theoretically uncorrelated with the local PRN code sequence:

$$\sum_{k=0}^{N-1} n_0 \times x(k) = N \times E[n_0 \times x(k)] = N \times E[n_0] \times E[x(k)] = 0. \tag{10}$$

Combining the above derivations, Re_{coef} is expressed as

$$Re_{coef} = \frac{z_{max}}{\sum\limits_{k=0}^{N-1} x^2(k)}. \tag{11}$$

This paper further introduces coherent accumulation to augment the correlation peaks of the received signal with the local PRN code. The magnitude of the correlation peaks is directly proportional to the accumulation of frames. Therefore, the above equation can be further modified as

$$Re_{coef} = \frac{z_{max}}{Acc_{num} \times \sum\limits_{k=0}^{N-1} x^2(k)}, \tag{12}$$

where Acc_{num} indicates the quantity of frames accumulated.

During our preliminary research, we discovered that the duration of a complete up-link DSSS signal packet, including the non-data-modulated section, data segment, and other components, is less than one second [1]. During the interval of signal continuity, the amplitude of the signal remains relatively stable, thereby enabling us to apply the amplitude estimation result derived from this method to the entire data packet.

Combining Equations (5) and (12), the reconstructed sequence used in this paper is

$$x(\hat{k}) = \frac{z_{max}}{Acc_{num} \times \sum_{k=0}^{N-1} x^2(k)} \times x(k). \tag{13}$$

4. Performance Analysis

In this section, the widely used Add White Gaussian Noise (AWGN) channel model and Monte Carlo method are adopted. We numerically evaluate the simulation results based on P_{cd} and BER to demonstrate the effectiveness of the proposed algorithm for the acquisition module. Moreover, we compare the performance of our proposed algorithm with the traditional correlation-based acquisition algorithm [26].

This simulation solely focuses on the analysis of interference caused by AWGN and MAI within an ideal Doppler environment. For the transmitters, each user utilizes a 2048-bit m sequence as the spreading code, which is generated by an 11-bit linear shift register. Subsequently, the spread spectrum signal is shaped and filtered using a root ascending cosine filter ($\alpha = 0.25$). After aliasing, the signals from the K users are received by the receiver via the AWGN channel. The system encounters multi-path delays, where the K users do not arrive at the on-board receiver simultaneously, yet possess the same transmit frequency. In the acquisition module, the improved algorithm is used to eliminate the effect of MAI on multi-user receivers.

In this analysis, we investigate the impact of the quantity of multi-user parallel communications on the acquisition process. Figure 7 illustrates the results, where an ISR of 20 dB is maintained and the number of users (K) ranges from 1 to 16. The interference-free scenario is used as a benchmark, represented by a dotted red dashed line. The traditional correlation-based acquisition algorithm is depicted by colored dashed lines. Notably, the P_{cd} of individual user acquisition is found to be very low, indicating that it fails to meet the requirements of satellite communication due to the presence of MAI. The proposed PIC-based acquisition algorithm, represented by colored solid lines, significantly enhances the P_{cd} for weak signals across the entire SNR range. Furthermore, no significant degradation in performance is observed for different values of K, with only minor variations evident in the mid-SNR range. In the high-SNR region, all curves achieve P_{cd} of 94%.

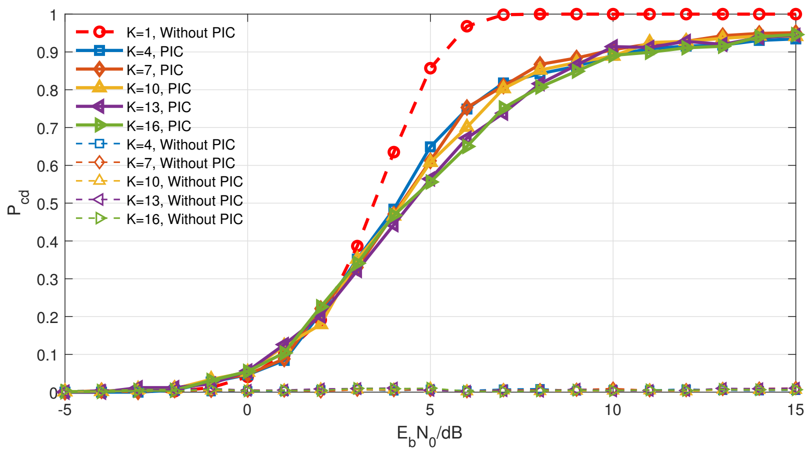

Figure 7. ISR = 20 dB, P_{cd} comparison of the proposed acquisition algorithm over AWGN channel.

In simpler terms, we discuss the impact of parameter ISR on the performance of the PIC-based acquisition algorithm. In Figure 8, we fixed the parameter K to 6 and varied the ISR from 5 to 30. When the ISR is below 20 dB, the performance of the algorithm is almost comparable to the theoretical limit. However, as the ISR increases, the performance of the algorithm gradually decreases across the entire SNR range. When the ISR exceeds 25 dB, even the improved algorithm struggles to meet the demands of satellite communication.

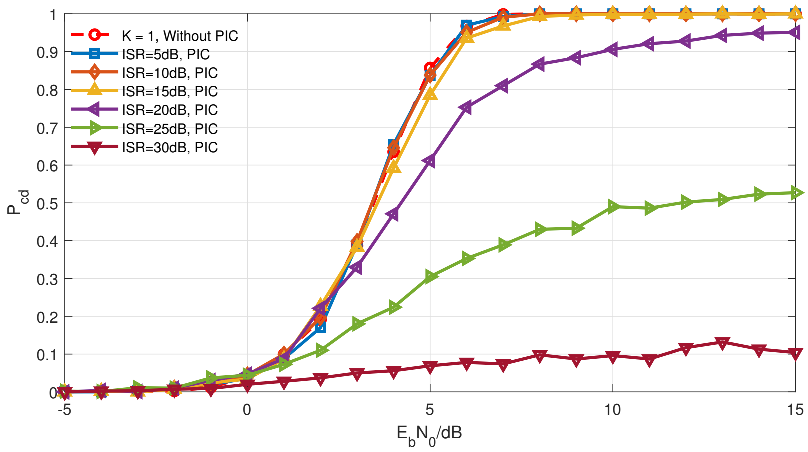

Figure 8. K = 6, P_{cd} of the proposed acquisition algorithm over AWGN channel.

On the other hand, we also analyze the effect of the parameters K (number of users) and ISR on the BER of the receiver, assuming successful acquisition. Similar to Figures 7 and 8, Figures 9 and 10 respectively analyze the effects of parameters K and ISR on the BER.

As shown in Figure 9, the ISR is fixed at 20 dB, and K is varied from 1 to 16. The BER theoretical curve serves as a benchmark, appearing as a dotted red dashed line. The outcomes of the improved and traditional algorithms are categorized into two groups: the improved algorithm is illustrated by colored solid lines, while the traditional algorithm is depicted by colored dashed lines. Curves with identical parameters are distinguished by matching colors and markers. Notably, when K equals 7, the system becomes greatly influenced by MAI, resulting in a degradation of 1.3 dB in the BER performance compared to the absence of interference. Subsequently, regardless of the increase or decrease in the number of users, the BER performance exhibits improvement. The introduction of the single-stage PIC algorithm elevates the BER of all curves by 0.8 dB.

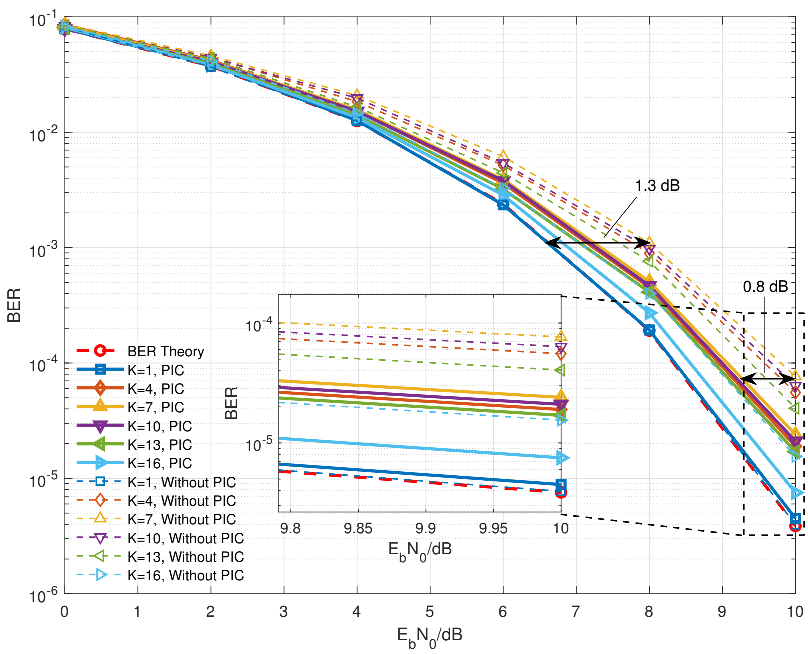

Figure 9. ISR = 20 dB, BER comparison of the proposed acquisition algorithm over AWGN channel.

In Figure 10, the relationship between ISR and BER is shown. As ISR increases, the BER also increases across the entire SNR range. However, the single-stage PIC algorithm effectively reduces the BER loss caused by MAI. When ISR is at 30 dB, the degradation caused by MAI can reach a maximum of 6.5 dB. After applying the single-stage PIC optimization, this degradation is reduced by 4 dB. Furthermore, the performance of the other curves is optimized by approximately 1 dB. The result shows that the PIC algorithm can enhance the BER of receivers. When ISR is less than 20 dB, the performance of the algorithm after single-stage PIC optimization approaches the theoretical limit as seen in Figure 8.

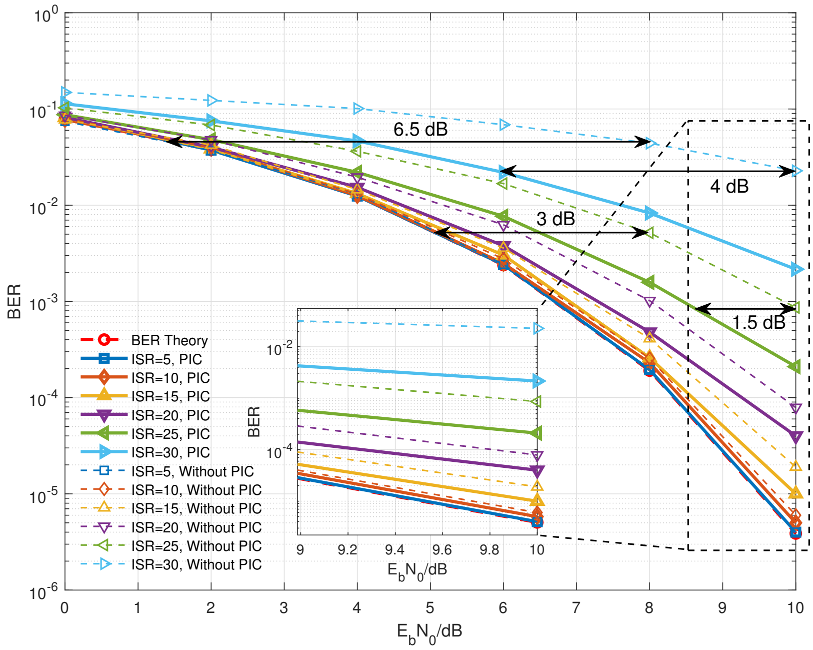

Figure 10. $K = 6$, BER comparison of the proposed acquisition algorithm over AWGN channel.

In conclusion, the proposed algorithm outperforms the traditional correlation-based acquisition algorithm in multi-user systems. When the ISR is below 20 dB, P_{cd} and BER are nearly equivalent to a no-interference environment. Additionally, the improved PIC algorithm reduces the BER of receivers by up to 4 dB compared to the correlation-based acquisition algorithm.

5. Hardware Experiment

To demonstrate the effectiveness of the proposed algorithm as well as its hardware feasibility, we constructed a hardware platform for testing. The topology and the photograph of this platform are presented in Figures 11 and 12. The main components of this platform are listed in Table 1.

Table 1. Main components of the hardware platform.

Identifier	Component	Model Specification
1	Multi-user transmitters FPGA	Xilinx xc7z020
2	Power combiner	Mini-Circuits ZB8PD-362-S+ Mini-Circuits ZB8PD-30-S+
3	Noise generator	Noise/com NC6110
4	Spectrum analyzer	Agilent 8563EC
5	Receiver FPGA	Xilinx xczu27dr
6	RF chip	AD9361

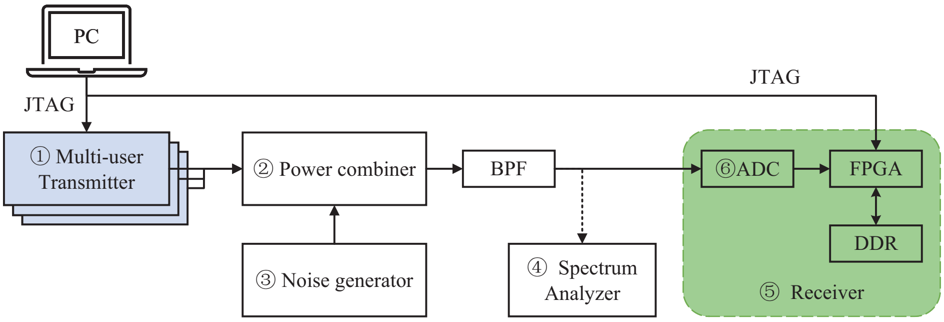

Figure 11. Topology of the hardware system.

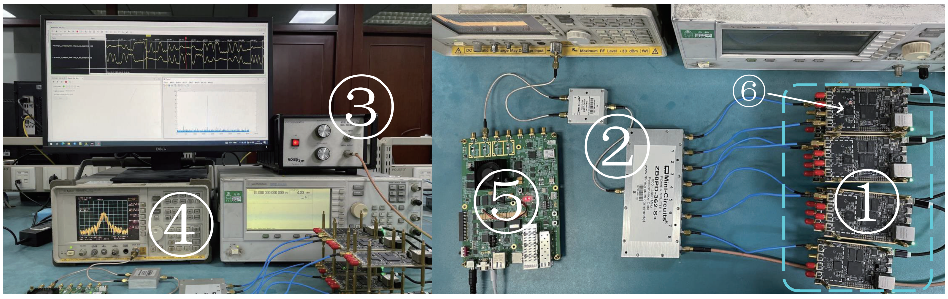

Figure 12. Photograph of the hardware system.

We employed ZYNQ-7000 integrated with AD9361 to construct our hardware transmitter. For this particular test, we utilized a total of seven transmitters, with one dedicated to transmitting the test signal and the remaining six for transmitting strong interference signals. To ensure compatibility, we developed transmission programs in the Verilog Hardware Description Language (Verilog HDL) on the aforementioned field programmable gate arrays (FPGAs). The transmitters accept I/Q baseband signals via a joint test action group (JTAG) table from our PC, subsequently modulating the baseband signal for transmission at a frequency of 2.25 GHz.

Then, the transmitting signals are merged with the output of a wide-band noise generator in consideration of the impact of AWGN. After passing through the filter, one of the output paths of the aliasing signal is directed towards a spectrum analyzer. The purpose of this analyzer is to quantify the power of the signal as well as the in-band noise, enabling the measurement of the SNR of the received signals.

The RF receiver is also constructed with ZYNQ-7000 and AD9361. To enhance the acquisition process, improved Verilog HDL acquisition programs are developed. With the assistance of ChipScope, we gather real-time processing outcomes from the acquisition program via a JTAG cable and utilize MATLAB for statistical analysis. To optimize data efficiency, we observe a substantial number of independent acquisition events, reaching up to 10^6 in total.

The modulation mode of the test signal and primary parameters are listed in Table 2, while the performance of BER is shown in Figure 13. The solid line represents the BER results of theoretical simulation, while the dashed line represents the results of hardware platform testing. The hardware implementation of the improved algorithm suffers a loss of 1.5 dB compared to the theoretical simulation, which is caused by the circuit chip process and AD chips. In addition, the hardware platform exhibits performance similar to simulation. The feasibility of the enhanced algorithm on hardware is established.

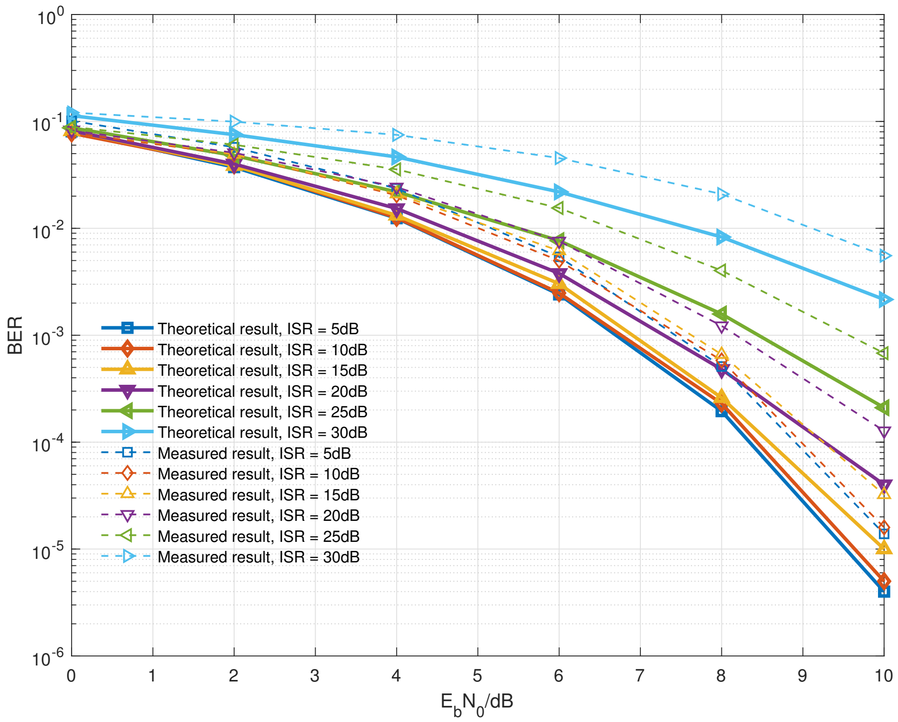

Figure 13. BER performance of the proposed acquisition receiver.

Table 2. System parameters.

Identifier	Parameter	Value
1	Modulation	BPSK
2	Shaping filter	Raised cosine filter
3	Spread spectrum ratio	2048
4	Oversample rate	20
5	Symbol rate	800 sps
6	Chip rate	1.6384 Mcps

6. Conclusions

In this paper, we presented an enhanced parallel acquisition algorithm that builds up the principles of PIC and coherent accumulation. Additionally, a signal hard reconstruction algorithm based on the acquisition result is also introduced. By combining the aforementioned algorithms, we effectively minimize the impact of MAI on multi-user spread spectrum communication systems. Compared to the traditional correlation-based algorithm, the improved algorithm significantly enhanced P_{cd} and raised BER by 1 dB, which meets the demand for satellite communication. Through extensive simulation and hardware testing, it is shown that our simulation, analysis, and experimental results are consistent. Specifically, we observed that P_{cd} can achieve 0.95 when ISR equals 20 dB caused by MAI. In summary, the MAI in multi-user DS-CDMA systems has an unavoidable impact and becomes more severe with an increase in the number of users. The algorithm proposed in this paper effectively eliminates MAI by reconstructing and parallel eliminating interference signals within the received signal, which enables the successful acquisition and reception of individual signals, making the algorithm applicable in various satellite communication systems.

Author Contributions: Conceptualization and methodology, H.L., X.D. and K.Y.; Software, H.L. and Y.J.; Validation, H.L. and D.Z.; Writing—original draft preparation, H.L., Y.J. and D.Z.; writing—review and editing, X.D. and K.Y.; Supervision, X.D. and K.Y. All authors have read and agreed to the published version of the manuscript.

Funding: This work was supported in part by the National Key Research and Development Program of China under Grant 2023YFC3305904, in part by the National Natural Scientific Foundation of China under Grants 62301049.

Data Availability Statement: Data are contained within the article.

Conflicts of Interest: The authors declare no conflict of interest.

References

1. Han, C.; Yang, Y.; Cai, Z. Beidou navigation satellite system and its time scales. *Metrologia* **2011**, *48*, S213. [CrossRef]
2. Shi, M.; Yang, K.; Niyato, D.; Yuan, H.; Zhou, H.; Xu, Z. The meta distribution of sinr in uav-assisted cellular networks. *IEEE Trans. Commun.* **2022**, *71*, 1193–1206. [CrossRef]
3. Hua, B.; Ni, H.; Zhu, Q.; Wang, C.X.; Zhou, T.; Mao, K.; Bao, J.; Zhang, X. Channel modeling for uav-to-ground communications with posture variation and fuselage scattering effect. *IEEE Trans. Commun.* **2023**, *71*, 3103–3116. [CrossRef]
4. Mao, K.; Zhu, Q.; Qiu, Y.; Liu, X.; Song, M.; Fan, W.; Kokkeler, A.B.; Miao, Y. A uav-aided real-time channel sounder for highly dynamic non-stationary a2g scenarios. *IEEE Trans. Instrum. Meas.* **2023**, *72*, 6504515. [CrossRef]
5. Ding, X.; An, J.; Zhao, Z.; Bu, X.; Yang, K. Low-density parity-check coded direct sequence spread spectrum receiver based on analog probabilistic processing. *IEEE Trans. Veh. Technol.* **2021**, *70*, 6355–6370. [CrossRef]
6. Fawer, U.; Aazhang, B. A multiuser receiver for code division multiple access communications over multipath channel. *IEEE Trans. Commun.* **1995**, *43*, 1556–1565. [CrossRef]
7. Murugesan, S.; Uysal-Biyikoglu, E.; Schniter, P. Optimization of training and scheduling in the non-coherent simo multiple access channe. *IEEE J. Sel. Areas Commun.* **2007**, *25*, 1446–1456. [CrossRef]
8. Lee, W.C. Overview of cellular cdma. *IEEE Trans. Veh. Technol.* **1991**, *40*, 291–302. [CrossRef]
9. Ding, X.; Zhou, K.; Li, G.; Gao, X.; Yuan, J.; An, J. Customized joint blind frame synchronization and decoding methods for analog ldpc decoder. *IEEE Trans. Commun.* **2023**. . [CrossRef]
10. Choi, K.; Cheun, K.; Jung, T. Adaptive pn code acquisition using instantaneous power-scaled detection threshold under rayleigh fading and pulsed gaussian noise jamming. *IEEE Trans. Commun.* **2002**, *50*, 1232–1235. [CrossRef]
11. Lee, Y.-H.; Kim, S.-J. Median-prefiltering-based robust acquisition of direct-sequence spread-spectrum signals in wide-band pulse jamming. *IEEE Trans. Veh. Technol.* **2002**, *51*, 171–179.
12. da Silva, C.; Milstein, L. Coarse acquisition performance of spectral encoded uwb communication systems in the presence of narrow-band interference. *IEEE Trans. Commun.* **2007**, *55*, 1374–1384. [CrossRef]
13. Wang, Y.; Wu, S. New acquisition decision algorithm for multiple access interference suppression in dsss system. *J. Syst. Electron.* **2011**, *22*, 157–163. [CrossRef]
14. Moshavi, S. Multi-user detection for ds-cdma communications. *IEEE Commun. Mag.* **1996**, *34*, 124–136. [CrossRef]
15. Xie, Z.; Short, R.T.; Rushforth, C.K. A family of suboptimum detectors for coherent multiuser communications. *IEEE J. Sel. Areas Commun.* **1990**, *8*, 683–690. [CrossRef]
16. Pan, J.; Ye, N.; Yu, H.; Hong, T.; Al-Rubaye, S.; Mumtaz, S.; Al-Dulaimi, A.; Chih-Lin, I. Ai-driven blind signature classification for iot connectivity: A deep learning approach. *IEEE Trans. Wirel. Commun.* **2022**, *21*, 6033–6047. [CrossRef]
17. Viterbi, A.J. Very low rate convolution codes for maximum theoretical performance of spread-spectrum multiple-access channels. *IEEE J. Sel. Areas Commun.* **1990**, *8*, 641–649. [CrossRef]
18. Kohno, R.; Imai, H.; Hatori, M.; Pasupathy, S. Combinations of an adaptive array antenna and a canceller of interference for direct-sequence spread-spectrum multiple-access system. *IEEE J. Sel. Areas Commun.* **1990**, *8*, 675–682. [CrossRef]
19. Rusch, L.A.; Poor, H.V. Multiuser detection techniques for narrowband interference suppression in spread spectrum communications. *IEEE Trans. Commun.* **1995**, *43*, 1725–1737 [CrossRef]
20. Varanasi, M.K.; Aazhang, B. Multistage detection in asynchronous code-division multiple-access communications. *IEEE Trans. Commun.* **1990**, *38*, 509–519. [CrossRef]
21. Kaplan, E.D.; Hegarty, C. *Understanding GPS/GNSS: Principles and Applications*; Artech House: Norwood, MA, USA, 2017.
22. Enge, P.K. The global positioning system: Signals, measurements, and performance. *Int. J. Wirel. Inf. Netw.* **1994**, *1*, 83–105. [CrossRef]
23. Zhao, L.; Gao, S.; Hao, Y. Improved fast fourier transform processing on fast acquisition algorithms for gps signal. In Proceedings of the 2009 9th International Conference on Electronic Measurement & Instruments, Beijing, China, 16–19 August 2009; pp. 4–221.
24. Ping, H.; Bing-fa, Z.; Hui, W. Pseudo noise code acquisition using fast fourier transform. In Proceedings of the 2008 International Symposium on Computer Science and Computational Technology, Shanghai, China, 20–22 December 2008; Volume 1, pp. 788–792.
25. Yang, L.; Tian, J. Analysis and compare of weak gps signal acquisition algorithms. In Proceedings of the IET International Communication Conference on Wireless Mobile & Computing (CCWMC 2009), Shanghai, China, 7–9 December 2009; pp. 492–495.

26. Tang, P.; Wang, S.; Li, X.; Jiang, Z. A low-complexity algorithm for fast acquisition of weak dsss signal in high dynamic environment. *GPS Solut.* **2017**, *21*, 1427–1441. [CrossRef]
27. Briskman, R.D. Radio determination satellite service. *Proc. IEEE* **1990**, *78*, 1096–1106. [CrossRef]